Temperature-Compensated High-Frequency Surface Acoustic Wave Device

Changjian Zhou, *Member, IEEE*, Yi Yang, Hualin Cai, *Student Member, IEEE*, Tian-Ling Ren, *Senior Member, IEEE,* Mansun Chan, *Fellow, IEEE*, and Cary Y. Yang, *Fellow, IEEE*

***Abstract*— We report high-frequency surface acoustic wave (SAW) devices with excellent temperature stability using a layered structure consisting of single-crystal $LiNbO_3$ thin film on $SiO_2/LiNbO_3$ substrate. SAW devices with a wavelength of 2 μm have been fabricated and several wave modes ranging from ~1.5 to 2.1 GHz have been obtained. With the SiO_2 interlayer providing the temperature compensation and the top single-crystal Z-cut $LiNbO_3$ piezoelectric thin film for acoustic wave excitation, the fabricated SAW devices exhibit excellent temperature coefficients of frequency. Theoretical calculations are presented to elucidate temperature compensation of the proposed layered structure.**

***Index Terms*— $LiNbO_3$ thin film, radio frequency, surface acoustic wave (SAW), temperature compensation.**

I. Introduction

TEMPERATURE stability is of great importance in high-frequency acoustic wave devices for telecommunication systems [1]–[3]. Quartz provides high temperature stability but very small electromechnical coupling coefficient K^2, which precludes itself as a candidate for radio frequency applications. Piezoelectric single-crystal $LiNbO_3$ (LN) and $LiTaO_3$ (LT) possess large K^2 but poor temperature stability. Commonly used piezoelectric materials have a negative temperature coefficient of frequency (TCF). Thus, one strategy is to integrate materials with a positive TCF with these piezoelectric materials for temperature compensation. In case of SAW devices, SiO_2 [1], [4], [5], TeO_2 [6], and AlN [7] overlays have been studied for temperature compensation. Among these materials, SiO_2 is the most commonly used material due to its easy accessibility and thickness suitable for temperature compensation at high frequency (>1 GHz). The TCF of the SiO_2/Al/LN-based SAW device is improved from −80 to −30 ppm/°C by this technique [4]. However, this configuration results in an uneven top surface, which deteriorates the performance of the temperature-compensated SAW devices. With optimization of the SiO_2 profile, the TCF is improved to be about −15 ppm/°C for LT-based SAW devices [5]. Further improvement in temperature stability would require precise control of the SiO_2 profile and optimization of the interdigital transducers (IDTs) in terms of material and thickness, which pose great challenge for both manufacturing process and device design.

In this letter, we demonstrate a novel single-crystal Z-cut LN thin film/SiO_2/LN (LN/SiO_2/LN) layered structure for temperature-stable high-frequency SAW devices. In comparison with the conventional structure, the proposed structure uses the SiO_2 interlayer but not the overlay for temperature compensation and the IDTs are directly formed on the top single-crystal LN thin film, thus precluding deterioration due to the uneven SiO_2 profile. Through combining a thin top LN layer and a relatively thicker SiO_2 compensating interlayer, the wave impinging upon the surface of the top LN layer will penetrate through the LN layer and also the SiO_2 interlayer. Thus, it is possible to achieve near-zero TCF for high-frequency SAW devices since the SAW energy distribution in the SiO_2 can be readily controlled. Further, the thermal expansion of the top LN layer is also suppressed due to the SiO_2 interlayer which has a near-zero coefficient of thermal expansion (CTE), also resulting in a smaller TCF. An excellent TCF (−2.34 ppm/°C at 2.13 GHz) is obtained for high-frequency SAW devices using the proposed layered structure. In the following sections, fabrication and characterization of the LN/SiO_2/LN SAW device are presented, and a theoretical analysis of its temperature compensation mechanism is presented.

II. Experiment

Fig. 1(a) shows the process flow for fabricating the LN/SiO_2/LN layered structure. The single-crystal LN thin film is transferred from the donor substrate to the handle substrate through ion implantation, wafer bonding, and splitting processes. The initial thickness of the LN thin film is determined by the depth of the ion implantation. For high-frequency SAW applications, very clean and atomically flat surfaces are required. Final polishing is then utilized to obtain

Manuscript received August 23, 2013; revised September 22, 2013; accepted September 22, 2013. Date of publication October 10, 2013; date of current version November 20, 2013. This work was supported in part by the National Natural Science Foundation under Grant 61025021, Grant 60936002, and Grant 61020106006, in part by the National Key Project of Science and Technology of China under Grant 2011ZX02403-002, and in part by the University Grant Council of the Government of HKSAR under Contract AoE/P-04/08. The review of this letter was arranged by Editor M. Tabib-Azar.

C. J. Zhou was with Institute of Microelectronics, Tsinghua University, Beijing 100084, China. He is now with the Department of Electronic and Computer Engineering, Hong Kong University of Science and Technology, Kowloon 999077, Hong Kong (e-mail: zhoucj86@gmail.com).

Y. Yang, H. Cai, and T.-L. Ren are with the Institute of Microelectronics, Tsinghua University, Beijing 100084, China (e-mail: rentl@tsinghua.edu.cn).

M. Chan is with the Department of Electronic and Computer Engineering, Hong Kong University of Science and Technology, Kowloon 999077, Hong Kong.

C. Y. Yang is with the Center for Nanostructures, Santa Clara University, Santa Clara, CA 95053 USA.

Color versions of one or more of the figures in this letter are available online at http://ieeexplore.ieee.org.

Digital Object Identifier 10.1109/LED.2013.2283305

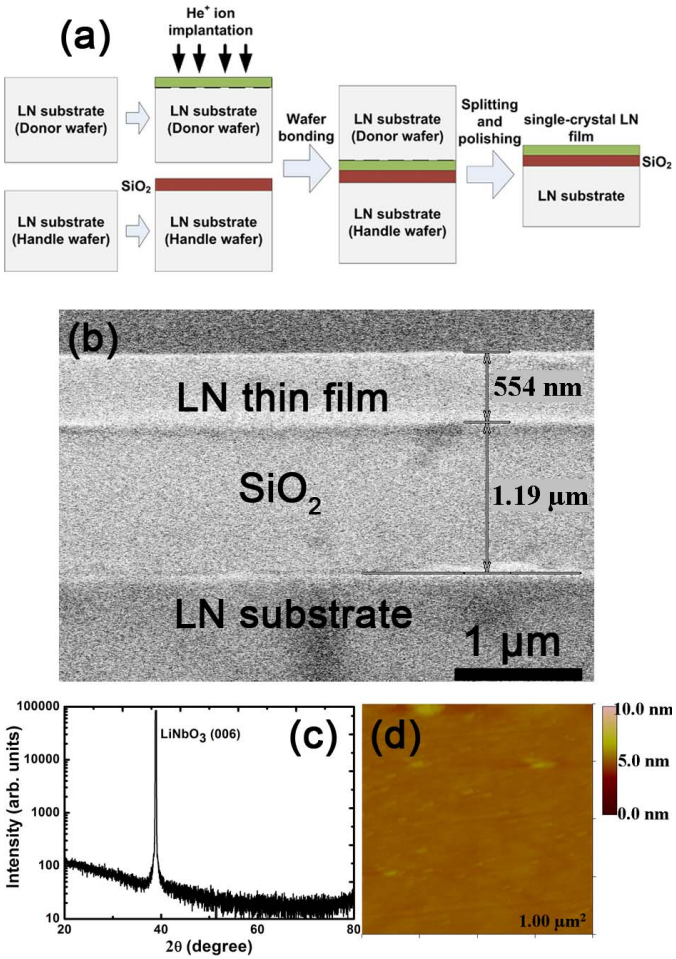

Fig. 1. (a) Fabrication process flow. (b) Cross-sectional SEM image of LN/SiO_2/LN layered structure. (c) XRD patterns of LN/SiO_2/LN structure, where only a strong (006) peak is observed. (d) AFM image of the top LN thin-film surface, with root mean square surface roughness of 0.28 nm over measured area of 1 μm^2.

a smooth surface and also to thin the film down to the required thickness. In this letter, the thicknesses of the top LN film and the SiO_2 interlayer are ~0.55 and 1.2 μm, respectively, [Fig. 1(b)]. The crystalline quality of the transferred LN layer is characterized by XRD measurements. The LN thin film exhibits a single strong (006) orientation with a full-width at half-maximum of 0.0468°, confirming its single-crystal property [Fig. 1(c)]. The root mean square surface roughness of the LN thin film is ~0.28 nm and no grain boundary is observed, as shown in Fig. 1(d).

The IDTs are formed on top of the LN thin film using E-beam lithography, Au/Ti (30/5 nm) evaporation, and lift-off processes. Each test device consists of 30 pairs of interdigital electrodes with an aperture of 100 μm. The nominal linewidth and pitch of the IDTs are both 0.5 μm, giving a SAW wavelength (λ) of 2 μm. Fig. 2 shows the SEM images of the test SAW device.

III. Results and Discussion

Electrical behaviors of the SAW device are characterized using a network analyzer with a temperature-controlled

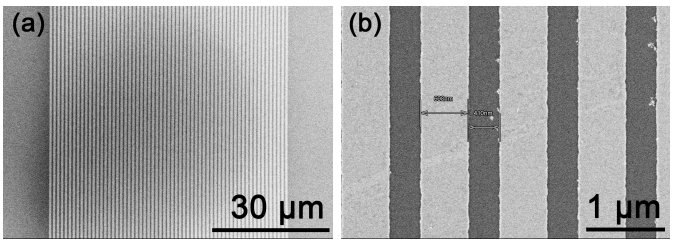

Fig. 2. SEM images of the SAW device showing. (a) 30 pairs of interdigital electrodes. (b) Close-up view of two electrode pairs.

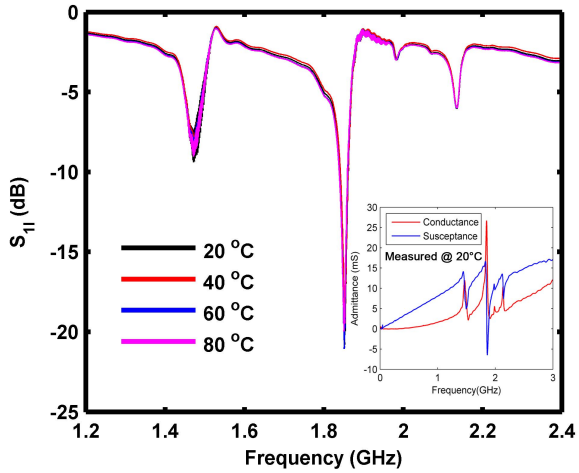

Fig. 3. S_{11} parameters of the SAW device measured from 20 °C to 80 °C. Inset: the admittance (conductance and susceptance) spectrum measured at 20 °C for K^2 extraction.

TABLE I
Experimental Results of the SAW Device on LN/SiO_2/LN Structure

f_c (GHz)	TCF (ppm/°C)	V_p (m/s)	K^2 (%)
1.4720	-6.79	2944.0	2.43
1.8527	-16.22	3705.4	4.89
2.1356	-2.34	4271.2	1.08

microwave probe station. Fig. 3 shows the reflection scattering parameters (S_{11}) of a fabricated SAW device measured from 20 °C to 80 °C. Table I summarizes the experimental results of the SAW device, including TCF, wave velocity (V_p), and K^2. The three wave modes with center frequencies (f_c) at 1.4720, 1.8527, and 2.1356 GHz, respectively, are examined in detail. The one with a center frequency at 1.980 GHz has a very low K^2 and is not suitable for practical application.

The TCF, defined as

$$\mathrm{TCF} = \frac{1}{f}\frac{\partial f}{\partial T} = \mathrm{TCV} - \mathrm{CTE} = \frac{1}{V_p}\frac{\partial V_p}{\partial T} - \mathrm{CTE} \quad (1)$$

depends on the temperature coefficient of velocity (TCV) and the CTE of the substrate. Experimentally, TCF is extracted from the calculated relative shifts of f_c. The proposed SAW device exhibits excellent temperature stability with the TCF improved from ~ −80 to −6.79, −16.22, and −2.34 ppm/°C, respectively, for the three wave modes. The wave velocities

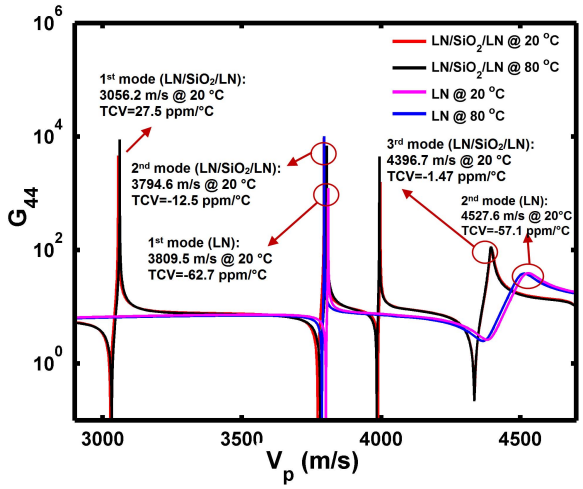

Fig. 4. Calculated Green's functions for LN/SiO_2/LN structure and LN substrate at 20 °C and 80 °C, with the wave velocities and TCVs indicated.

are readily obtained as $V_p = f_c \times \lambda$. K^2 is given by $K^2 = \pi G_m(f_0)/4NB_s(f_0)$ [8], where N is the IDT finger pairs and equals to 30 in this letter, f_0 corresponds to the frequency where the conductance of the IDT reaches the maximum value, $G_m(f_0)$ and $B_s(f_0)$ are the motional conductance and static susceptance of the IDT at f_0 and can be extracted from the admittance parameter obtained from S_{11}. Inset of Fig. 3 shows the spectrum of the admittance (conductance and susceptance) from which K^2 is computed. The results are summarized in Table I.

To examine temperature compensation of the proposed LN/SiO_2/LN layered structure, the acoustic wave velocities of the wave modes and corresponding TCVs are calculated using the scattering matrix method [9]. The plane wave propagated in the layered structure is described as the superimposition of eight partial waves, with each being incident or reflected wave depending on whether the partial wave is increasing or decreasing with depth inside the layer. Given the normalized thickness (h/λ) of each layer in the structure, the propagation mode velocity V_p is then determined by locating the poles of the Green's matrix element G_{44} obtained by the scattering matrix method. Fig. 4 shows the calculated G_{44} of the LN($h/\lambda = 0.275$)/SiO_2($h/\lambda = 0.6$)/LN layered structure and the LN substrate at 20 °C and 80 °C, considering temperature dependence of the material constants of LN and SiO_2 [10]–[12]. In general, the deviations of the theoretical velocities from the experimental ones are <4% for all the wave modes, indicating the high accuracy of this calculation. The two modes excited in the LN substrate exhibit a theoretical TCV of −62.7 and −57.1 ppm/°C, respectively. In comparison, the three modes excited in the LN/SiO_2/LN structure exhibit calculated TCV values of 27.5, −12.5, and −1.47 ppm/°C, respectively. These values further confirm the superior temperature stability of the proposed structure. For the first mode in LN/SiO_2/LN, the calculated TCV is positive with a larger magnitude than the experimental TCF. The lower velocity of the first mode indicates that the wave energy is more confined in the SiO_2 interlayer and its temperature compensation might be overestimated as a result. For the second and third wave modes, the theoretical TCV values compare well with their experimental TCF counterparts, with the small discrepancies attributed mainly to CTE.

Unlike the LN substrate in which CTE is constant (15.4 ppm/°C), CTE of the layered structure depends on the specified wave mode and thicknesses of each layer. In general, because of the small CTE of SiO_2 (0.54 ppm/°C) and the relatively thicker SiO_2 interlayer (0.6 λ) than the commonly used SiO_2 overlayer (0.2 $\sim$ 0.3 λ), the proposed layered structure can exhibit a smaller CTE than the LN substrate and other temperature-compensated layered structure. That is another reason for the excellent TCF obtained for the LN/SiO_2/LN structure.

IV. Conclusion

We have presented the first implementation of a single-crystal LN/SiO_2/LN layered structure for high-frequency SAW devices with excellent temperature stability. Significant improvements in TCF have been obtained for SAW devices with working frequencies >1.5 GHz. Theoretical calculations have been performed to identify the physical origins of temperature compensation in the proposed structure. It is found that both TCV and CTE of the proposed layered structure are lower than those in existing SAW devices, thus resulting in excellent temperature stability.

References

[1] K. Hashimoto, M. Kadota, T. Nakao, *et al.*, "Recent development of temperature compensated SAW devices," in *Proc. IEEE IUS*, Oct. 2011, pp. 79–86.

[2] H. Yu, W. Pang, H. Zhang, *et al.*, "Ultra temperature-stable bulk-acoustic-wave resonators with SiO_2 compensation layer," *IEEE Trans. Ultrason., Ferroelect., Freq. Control*, vol. 54, no. 10, pp. 2102–2109, Oct. 2007.

[3] H. Campanella, L. Khine, and J. M. Tsai, "Aluminum nitride Lamb-wave resonators for high-power high-frequency applications," *IEEE Electron Device Lett.*, vol. 34, no. 2, pp. 495–497, Feb. 2013.

[4] H. Nakamura, H. Nakanishi, T. Tsurunari, *et al.*, "Miniature surface acoustic wave duplexer using SiO_2/Al/$LiNbO_3$ structure for wide-band code-division multiple-access system," *Jpn. J. Appl. Phys.*, vol. 47, no. 5, pp. 4052–4055, May 2008.

[5] R. Takayama, H. Nakanishi, Y. Iwasaki, *et al.*, "Study of relationship between layer profile of SiO_2 and characterizatics of surface acoustic wave devices in SiO_2/Al/$LiTaO_3$ system," *Jpn. J. Appl. Phys.*, vol. 50, no. 7, pp. 07HD12-1–07HD12-6, Jul. 2011.

[6] N. Dewan, M. Tomar, V. Gupta, *et al.*, "Temperature stable $LiNbO_3$ surface acoustic wave device with diode sputtered amorphous TeO_2 over-layer," *Appl. Phys. Lett.*, vol. 86, no. 22, pp. 223508-1–1223508-3, May 2005.

[7] G. Bu, D. Ciplys, M. S. Shur, *et al.*, "Leaky surface acoustic waves in Z-$LiNbO_3$ substrates with epitaxial AlN overlays," *Appl. Phys. Lett.*, vol. 85, no. 15, pp. 3313–3315, Oct. 2004.

[8] C. Zhou, Y. Yang, J. Zhan, *et al.*, "Surface acoustic wave characteristics based on c-axis (006) $LiNbO_3$/diamond/silicon layered structure," *Appl. Phys. Lett.*, vol. 99, no. 22, pp. 022109-1–022109-3, Jul. 2011.

[9] A. Reinhardt, T. Pastureaud, S. Ballandras, *et al.*, "Scattering matrix method for modeling acoustic waves in piezoelectric, fluid and metallic multilayers," *J. Appl. Phys.*, vol. 94, no. 10, pp. 6923–6931, Nov. 2003.

[10] R. T. Smith and F. S. Welsh, "Temperature dependence of the elastic, and dielectric constants of lithium tantalate and lithium niobate," *J. Appl. Phys.*, vol. 42, no. 6, pp. 2219–2230, May 1971.

[11] K. E. Petersen, "Dynamic micromechanics on silicon: Techniques and devices," *IEEE Trans. Electron Devices*, vol. 25, no. 10, pp. 1241–1250, Oct. 1978.

[12] B. Ivira, P. Benech, R. Fillit, *et al.*, "Modeling for temperature compensation and temperature characterizations of BAW resonators at GHz frequencies," *IEEE Trans. Ultrason., Ferroelect., Freq. Control*, vol. 55, no. 2, pp. 421–430, Feb. 2008.